JOURNAL OF PROPULSION AND POWER
Vol. 23, No. 5, September–October 2007

# Chemical Speciation of Hydrocarbon Emissions from a Commercial Aircraft Engine

Paul E. Yelvington,* Scott C. Herndon,† Joda C. Wormhoudt,† John T. Jayne,† and Richard C. Miake-Lye‡
*Aerodyne Research, Inc., Billerica, Massachusetts 01821*
W. Berk Knighton§
*Montana State University, Bozeman, Montana 59717*
and
Changlie Wey¶
*QSS Group, Inc., Cleveland, Ohio 44135*

DOI: 10.2514/1.23520

**In April 2004, the Aerodyne Mobile Laboratory measured trace gas and particle emissions from a CFM56-2C1 high-bypass-ratio turbofan engine used to power the NASA DC-8 aircraft as part of the Aircraft Particle Emissions Experiment (APEX). This article focuses on the measured hydrocarbon species which include formaldehyde, ethylene, acetaldehyde, benzene, toluene, and several higher aromatic species. Formaldehyde and ethylene were measured by tunable-infrared-laser differential absorption spectroscopy, and the other species were measured by proton-transfer reaction mass spectroscopy. Continuous samples were taken at 1, 10, and 30 m downstream of the engine-exit plane of the grounded aircraft and analyzed at a frequency of up to 1 Hz. The engine power was scanned from ground-idle up to takeoff power, and three fuel types (a baseline JP-8, a high-aromatic fuel, and a high-sulfur fuel) were investigated. Fuel type and plume age were shown to have only a minor impact on hydrocarbon emissions within the ranges studied in this experiment. However, ambient temperature was shown to have a substantial effect on these emissions. The sum of these speciated measurements agreed favorably with separate measurements of the total hydrocarbon emissions by flame ionization. The fast time response of the speciated measurements revealed interesting variability and transient behavior on a several-second timescale.**

## Introduction

MEASUREMENTS of total hydrocarbons from commercial aircraft engines, which are required for certification by the International Civil Aviation Organization (ICAO), have been reported for a broad range of engines [1]. However, measurements of individual chemical species which contribute to the total hydrocarbon emissions are rare. These speciated measurements are important for understanding the impact of air travel on global climate and local air quality [2–4]. The most comprehensive previous study of speciated hydrocarbons was performed by Spicer et al. [5,6], who studied ten turbine engines in the 1980s including the CFM56 engine. Those experiments examined grab samples of aircraft exhaust using gas chromatography. Slemr et al. [7] measured a number of hydrocarbon species from an in-flight DLR research aircraft using Fourier-transform infrared spectroscopy. Vay et al. [8] also measured trace gases, including CO and $CH_4$, from several in-flight aircraft using differential laser absorption. More recently, Anderson et al. [9] measured hydrocarbons from the Rolls Royce RB211 turbofan engine using grab sampling and gas chromatography. Also recently, Herndon et al. [10] measured formaldehyde, acetaldehyde, benzene, and toluene, as well as other hydrocarbons, from in-use aircraft at Boston Logan airport using tunable-infrared-laser differential adsorption spectroscopy (TILDAS) and proton-transfer reaction mass spectroscopy (PTR-MS).

This study represents the first real-time, ground-level measurements of speciated hydrocarbon emissions from a dedicated commercial aircraft engine. A good deal of information about the variability and transient nature of these emissions is available from these measurements because of the fast response time of the instruments. Also, ground-level tests allow a detailed examination of different power conditions in addition to the cruise conditions studied during in-flight measurements. Results are represented as emissions indices (mass of pollutant formed per mass of fuel consumed), which are deduced from the hydrocarbon concentrations and the measured concentration of $CO_2$ from a nondispersive infrared instrument.

The instruments and sampling system are briefly discussed in the Experimental Section along with a discussion of the data analysis procedure. The Results and Discussion section describes the effect of fuel type, downstream distance, and engine power on hydrocarbon emission indices. Also discussed is the variability in measured hydrocarbons, the interfering effects of ambient temperature, and the transient behavior of these emissions during changes in engine power.

A detailed description of the APEX measurement campaign and sampling system is presented elsewhere [11]. More details about the PTR-MS measurement procedure and analysis of data are given by Knighton et al. [12]. Concurrent measurements of nitrogen oxides [13] and particulate species [14] using the Aerodyne Mobile Laboratory are addressed in separate publications.

## Experimental Section

During 23–29 April 2004 the Aerodyne Mobile Laboratory was parked on a pad at Dryden Field on Edwards Air Force Base (Mojave Desert, California) next to the NASA DC-8 aircraft and

Received 27 February 2006; revision received 20 December 2006; accepted for publication 4 February 2007. 

*Principal Engineer, 45 Manning Road.
†Principal Scientist, 45 Manning Road.
‡Principal Scientist and Center Director, 45 Manning Road. AIAA Member.
§Research Associate Professor, Department of Chemistry and Biochemistry, P.O. Box 173400.
¶Senior Research Scientist, 21000 Brookpark Road.

approximately 100 ft from the CFM56-2C1 engine that was measured. Trailers belonging to other researchers including the University of Missouri–Rolla, Arnold Engineering Development Center, and U.S. Environmental Protection Agency were lined up next to the Aerodyne vehicle. The airplane remained grounded and stationary during these tests. Sample gases were taken continuously from different positions downstream of the engine exit. Three fuels were examined: 1) a baseline JP-8 fuel from Edwards Air Force Base, 2) a high-sulfur fuel (1600 ppmm sulfur) obtained by doping the baseline fuel with tertiary butyl disulfide, and 3) a high-aromatic Jet A fuel purchased from a California refinery. Sampling, measurement, and data analysis procedures used during APEX are described next.

#### Sampling System

Probe stands were located at 1, 10, and 30 m downstream of the engine-exit plane. The 1 and 10 m probe stands supported rakes of six conventional gas probes and six dilution probes aligned vertically. After some preliminary testing of the spatial variability of the emissions, one central probe tip was selected for the 1 and 10 m probe rakes. All speciated hydrocarbon measurements reported here used samples drawn from the dilution probes, however, the total hydrocarbon measurements used samples drawn from the gas probes. The stainless steel sample lines running from the dilution probes were unheated and the majority of the approximately 100 ft of line length was $\frac{3}{4}$-in.-o.d. tubing. The sample gas was diluted at the probe tip with dry nitrogen to a dilution ratio of approximately 10:1. Even for the most challenging sampling conditions (i.e., 1 m downstream location and takeoff power), the dilution gas quickly reduces the sample gas temperature to <150°C based on simple thermodynamic calculations, and so measurement bias caused by chemical conversion in the sampling system is expected to be minimal. Two valve boxes were used to select (or gang) the probe tips and to distribute the sample gas among researchers. The 30 m probe stand consisted of a single undiluted probe tip and a $\frac{3}{4}$-in.-o.d. unheated stainless steel sample line. The sample residence times were estimated by bulk-flow calculations to be 6.2 s (1 m probe), 5.4 s (10 m probe), and 2.7 s (30 m probe) [15].

#### Gaseous Measurements

Formaldehyde (HCHO) and ethylene ($C_2H_4$) were measured by tunable-infrared-laser differential absorption spectroscopy. The TILDAS instrument directs an infrared laser beam through a multipass cell and onto a detector. The light source was a tunable lead-salt diode laser (TDL) for the HCHO measurement and a quantum-cascade laser (QCL) [16,17] for the $C_2H_4$ measurement. The frequency of the lasers was swept over a narrow region of the spectrum (<1 $cm^{-1}$) at a high-repetition rate (>3 kHz). Features of the resulting rotational–vibrational transmission spectra were fit to a Voigt line-shape model using line strengths and other line parameters from Herndon et al. [18] for HCHO or the high-resolution transmission molecular absorption (HITRAN) database [19] for $C_2H_4$. The spectral feature used to measure HCHO was located at 1725.8 $cm^{-1}$, and several individual features in the range of 954–958 $cm^{-1}$ were used to measure $C_2H_4$ on different days of the experiment. The 1 s root mean square (rms) precision for these measurements was 700 pptv (HCHO) and 2 ppbv ($C_2H_4$). Numerous factors influence the accuracy of these measurements, including the laser line width, interferences in the transmission spectra from other species, and uncertainties in the reported line strengths used to fit the spectra. The laser line widths for these experiments (<0.001 $cm^{-1}$) were acceptably narrow, and the most significant spectral interference reported in the HITRAN database was approximately 1000 times smaller than the features of interest, and so the largest source of error is believed to be the uncertainty in the reported line strengths. Smith et al. [20] report estimated uncertainties of 7% (HCHO) and <10% ($C_2H_4$) for these compounds and these values give an idea of the accuracy of these measurements. The response time of this instrument is determined by the flow rate through the sample cell under the conditions of this experiment and is estimated to be approximately 1 s.

Acetaldehyde, benzene, toluene, and other aromatic compounds were measured by proton-transfer reaction mass spectrometry. The PTR-MS (Ionicon Analytic, GmBH) employs a chemical ionization mass spectrometer that uses hydronium ions ($H_3O^+$) to ionize species in the sample gas that are then mass selected and analyzed by a quadrupole mass spectrometer. The $H_3O^+$ ions transfer an $H^+$ via proton-transfer reactions to species having a proton affinity greater than that of water. Species present in aircraft exhaust which meet this criterion for detection by PTR-MS include unsaturated hydrocarbons, carbonyls, and aromatics. Aromatic species are particularly well resolved by PTR-MS because they resist fragmentation when ionized and have little interference at the mass-to-charge ratios where they are detected. The assignment of species to mass-to-charge (m/z) ratios drew on measurements of fragmentation patterns, proton affinities, and prior gas chromatographic analysis of exhaust from a CFM56 engine performed by Spicer et al. [6]. Some m/z ratios cannot be attributed to a single chemical species and in those cases the several species most likely to contribute to that signal are given. Twenty-one signals have been attributed to 26 chemical species (or sets of isomers) using PTR-MS including propene, acetaldehyde, benzene, and toluene. The detection limit, defined as three times the rms precision of a measured background signal, was found to be in the range of 0.3–1.2 ppbv for the compounds reported here. The detection limits of methanol (2.8 ppbv), propene (3.4 ppbv), acetaldehyde (2.7 ppbv), and acetic acid (3.4 ppbv) are slightly higher due to higher persistent instrument noise for these ion masses. The time response of the PTR-MS was approximately 4 s during this measurement campaign.

Carbon dioxide ($CO_2$) was measured using a commercial nondispersive infrared instrument (LI-COR 6262) to allow calculation of emission indices for the measured hydrocarbons. The published calibration range of this instrument is 0–3000 ppmv, and the manufacturer's quoted accuracy is ±0.5% under the conditions of this experiment. The LI-COR instrument was calibrated with an 800 ppmv gas standard tank. Occasionally the $CO_2$ mixing ratio in the diluted exhaust stream exceeded 3000 ppmv, and in those cases a correction was applied to the LI-COR-measured mixing ratio based on a high-range $CO_2$ measurement performed by NASA Langley Research Center. This correction was always less than 5% (the value at 5000 ppmv) and usually less than 3% (the value at 4000 ppmv). The time response for the LI-COR instrument was approximately 1 s.

#### Data Analysis

The emission index (mass pollutant formed per mass fuel consumed) is the accepted form for reporting emissions from aircraft and it is calculated using the following formula.

$$\mathrm{EI}_x[\mathrm{g}\,x/\mathrm{kg\ fuel}] = \mathrm{ER}_x[\mathrm{mol}\,x/\mathrm{mol\,CO_2}](\mathrm{MW}_x/\mathrm{MW}_{\mathrm{CO_2}})(3160\ \mathrm{g\,CO_2/kg\ fuel}) \quad (1)$$

Equation (1) uses above-ambient concentrations of $CO_2$ as a tracer for the exhaust plume [21–23]. The conversion factor of 3160 g $CO_2$/kg fuel is based on complete combustion of a jet fuel with a C/H ratio of 1.9 and is good to three significant figures for the fuels used in this experiment. Because the combustion efficiency of the measured CFM56 engine was always greater than 96% and usually greater than 99%, the error associated with assuming complete combustion is small. The emission ratio (ER) can be calculated in one of two ways. First, a simple average (corrected for background signals) can be computed over the time period corresponding to a given experimental condition using

$$\mathrm{ER}_x = \frac{\bar{c}_x - c_{x,b}/d}{\bar{c}_{\mathrm{CO_2}} - c_{\mathrm{CO_2},b}/d} \quad (2)$$

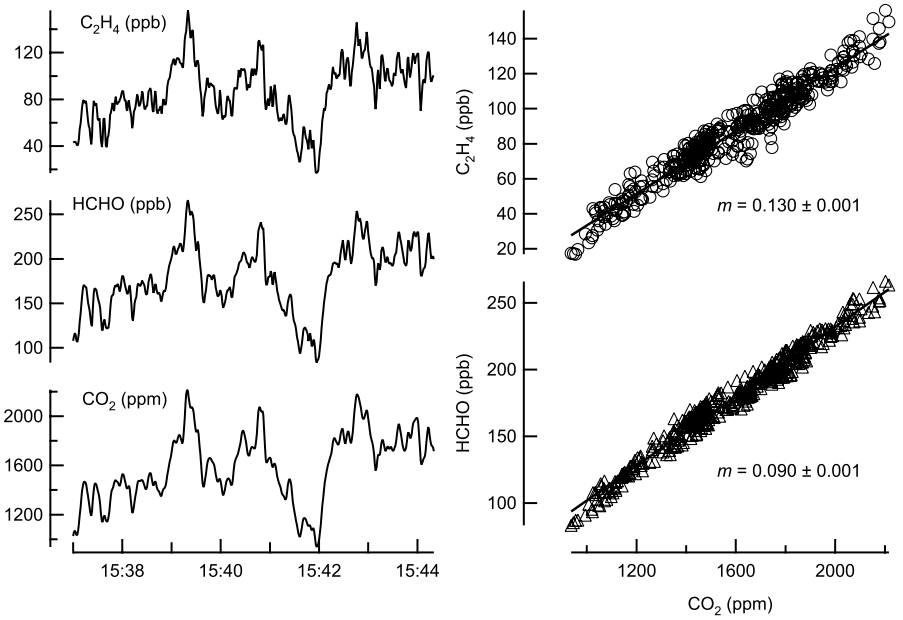


**a) Temporal data stream (archived at 1 Hz)** **b) Correlation between HCHO, $C_2H_4$, $CO_2$ ($m$=slope ± σ)**

**Fig. 1 Concentration of HCHO, $C_2H_4$, and $CO_2$ sampled at 10 m downstream of engine-exit plane (7% engine power; high-sulfur fuel).**

where $\bar{c}_x$ and $\bar{c}_{CO_2}$ are the average concentrations of species $x$ and $CO_2$, $c_{x,b}$ and $c_{CO_2,b}$ are the background concentrations of species $x$ and $CO_2$, and $d$ is the dilution ratio in the sample line. Because the background concentrations of HCHO and $C_2H_4$ are small compared with the levels in the aircraft exhaust, the $c_{x,b}$ term was neglected. For the 1 m probe location, the correction for background $CO_2$ was also neglected because it is of minor importance. As a result, the dilution ratio $d$ was not needed for the 1 m data. Also, the 30 m probe was not diluted, and so $d = 1$ for that data. For the 10 m probe, $d$ was estimated by comparing the measured $CO_2$ concentration to an average undiluted $CO_2$ concentration 10 m downstream of the engine at the specified engine power.

An alterative to this averaging method is to plot $c_x$ vs $c_{CO_2}$ and perform a linear least-squares regression; the resulting slope being an estimate of $ER_x$. This approach, which has recently been applied to advected aircraft plume measurements by Herndon et al. [24], has two potential advantages. First, apparent variability in the measured mixing ratios caused by changing winds is removed. As a result, the calculated uncertainties are a better measure of the variability in the instrument and emissions source rather than the weather conditions. Second, the dilution ratio and background concentrations are not needed for this method. Figure 1 demonstrates the slope method of determining emission ratios for a 7 min period of data from the 10 m probe when the engine was at idle (7% engine power). Notice that the $CO_2$ concentration varies over a substantial range from 1000 to 2200 ppmv and the accuracy of the slope is quite good. This wind-induced variability is not seen for the 1 m probe, and so the averaging method is used exclusively to analyze that data. The slope method can also give least-squares fits of unsatisfactory accuracy at the 10 and 30 m locations when the winds are steady. For this data set, the slope method was only used when the Pearson's $R$ value was greater than 0.75. This criterion resulted in standard deviations ($\sigma$) of the slope that were always smaller than the standard deviation resulting from the averaging method, which was obtained by propagating the uncertainties in the $CO_2$ and hydrocarbon mixing ratios.

It should be noted that the ER calculated by the two methods agree quite well, and only the error bars are noticeably different because the slope method removes artificial variability caused by the wind. This remark is addressed by Fig. 2, which shows a parity plot comparing the methods. The horizontal error bars (averaging method) are larger than the vertical error bars (slope method), but the regression line is quite close to the line $y = x$.

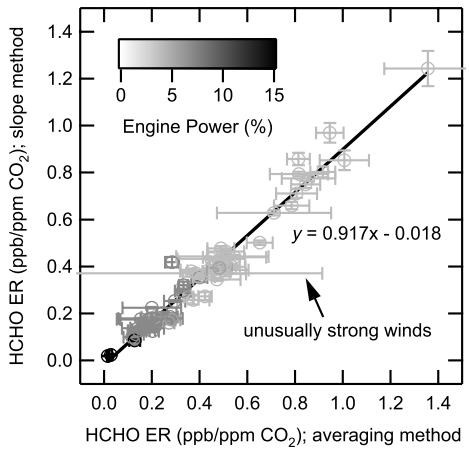


**Fig. 2 Comparison of HCHO emission ratio calculated by two methods (10 and 30 m downstream; all fuels).**

## Results and Discussion

### Effect of Fuel and Downstream Distance

Fuel type was not expected to have a significant effect on hydrocarbon emission indices because of the similar C/H ratios of the fuels, and that was confirmed by this data set. Downstream distance in the range studied (1–30 m) also did not have a noticeable effect on hydrocarbon emissions. Figure 3 demonstrates these observations by showing the emission ratio of HCHO, generally the most abundant hydrocarbon in aircraft exhaust, as a function of distance downstream and fuel type at 4% engine power (ground idle). The data points are shaded by ambient temperature, which varied in the range of 11–34°C during the measurements, and this shows a strong correlation between temperature and the emission ratio of formaldehyde. Any small dependence of hydrocarbon emissions on distance downstream or fuel type is obscured by the effect of ambient temperature. Figure 4 shows the dependence of $ER_{HCHO}$ on ambient temperature explicitly for three engine power settings. Most likely, the ambient temperature $T_{amb}$ is affecting the hydrocarbon emissions by influencing $T_3$, the combustor-inlet temperature. Combustion efficiency generally increases with increasing $T_3$, which is directly proportional to $T_{amb}$. And so, it is reasonable that hydrocarbon emission indices decrease with increasing ambient temperature, and

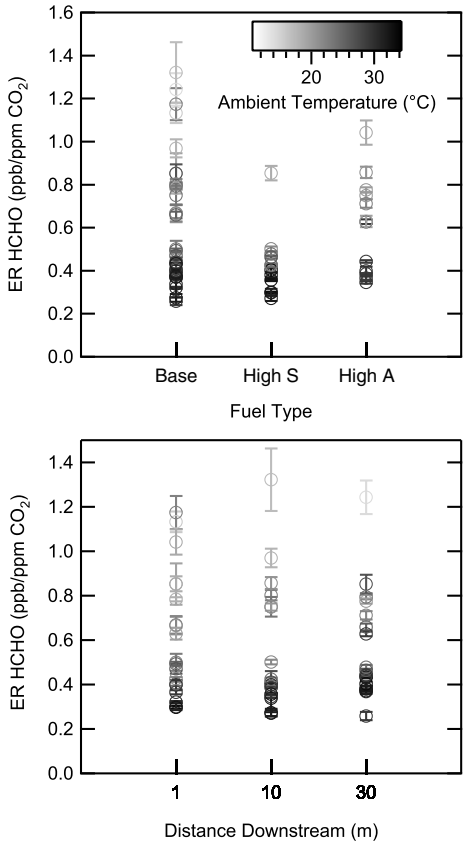


**Fig. 3 Emission ratio of formaldehyde at ground idle plotted vs distance downstream and fuel type.**

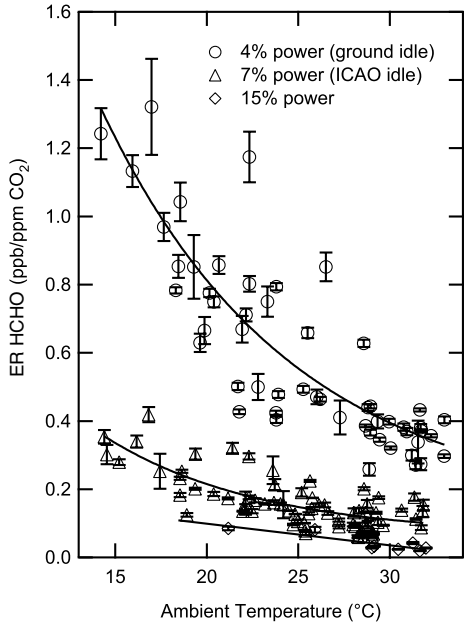


**Fig. 4 Effect of ambient temperature on formaldehyde emission ratio for three engine powers (all fuels; all downstream distances).**

it is noteworthy that the temperature effect is greater than two of the factors explored under this campaign.

### Variation with Engine Power

Spicer et al. [5,6] and others have shown that hydrocarbon emissions from aircraft are a strong nonlinear function of engine power. This behavior was also observed for the CFM56 engine during these measurements. Figure 5 shows that the HCHO emission

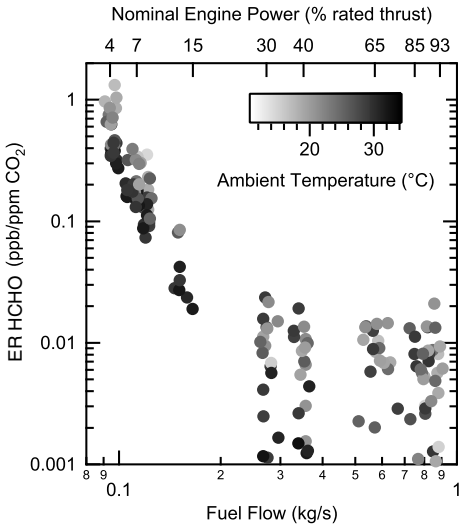


**Fig. 5 Variation of formaldehyde emission ratio with fuel flow (or engine power) for the CFM56-2C1 engine.**

ratio decreased by two orders of magnitude as the engine power is increased from 4% power (ground idle) to 93% power (takeoff). The scatter in the data at high engine powers (>30%) show that the HCHO mixing ratios were approaching the detection limit of the TILDAS instrument, as operated at APEX. At low engine power ($\leq$ 15%), fluctuations in ambient temperature appear responsible for some of the variability in the data, however, the effect of engine power was larger than that of ambient temperature. The top axis shows several of the nominal power conditions sampled during the APEX campaign and the lower axis shows the fuel flow rate. The horizontal scatter in the data points shows that the fuel flow rate for a given nominal power condition varied for the different test cycles. This variability in fuel flow likely contributes to the observed scatter in Figs. 3 and 4 in addition to variability in ambient temperature. The behavior of the other hydrocarbons was qualitatively similar to that of HCHO.

### Speciation of Engine Exhaust

This section summarizes all the hydrocarbon emissions that were measured by the TILDAS and PTR-MS instruments during the APEX measurement campaign. Because the effects of downstream distance and fuel type on hydrocarbon emissions were not significant relative to the temperature effect, the data were averaged over all fuels and all probe locations. Table 1 shows 20 hydrocarbon emissions at 4, 5.5, 7, and 15% engine power. The emissions reported in the table are averages over several measurement periods, and the standard deviations and fractional errors are also given. The reported uncertainty quantifies variability caused by the ambient conditions, engine operating conditions, and measurement precision. The emissions at engine powers greater than 15% were usually below the detection limit of the instruments, as operated at APEX. When an ion mass from the PTR-MS could not be assigned to a single hydrocarbon compound, the set of compounds or isomers corresponding to that ion mass is given. The results are presented as a carbon emission ratio $ER_C$ (moles of carbon in a given HC emitted per mole of $CO_2$ produced), which was calculated by multiplying the ER calculated by Eq. (2) by the number of C-atoms per hydrocarbon $N_C$. [To calculate the emission index, divide $ER_C$ values from Table 1 by $N_C$ and use the resulting ER in Eq. (1).] For ion masses where the number of carbons per molecule is not clear (e.g., m/z 57 can be $C_3H_4O$ or $C_4H_8$), $N_C$ was assigned based on the more abundant species as measured by Spicer et al. [6] for the CFM56 engine. Because the combustion efficiency of the engine is always close to unity, the carbon emission ratio (units of ppbC HC/ppm $CO_2$) is essentially 1000 times the fraction of carbon atoms in the fuel that are emitted as a given hydrocarbon. In terms of carbon emission ratio, ethylene is the most abundant hydrocarbon at

**Table 1 Hydrocarbon speciation for the CFM56-2C1 engine (all fuels; all downstream distances) as carbon emission ratios (ppbC/ppm $CO_2$)**

| Species or signal | Engine power, % rated thrust | | | |
|---|---|---|---|---|
| | 4% | 5.5% | 7% | 15% |
| HCHO[a] | 0.6 ± 0.3 (46%) | 0.22 ± 0.09 (39%) | 0.16 ± 0.08 (48%) | 0.04 ± 0.03 (61%) |
| $C_2H_4$[b] | 1.0 ± 0.5 (47%) | 0.4 ± 0.3 (82%) | 0.2 ± 0.4 (187%) | —— |
| m/z 41[c,d] | 0.2 ± 0.1 (53%) | 0.09 ± 0.03 (36%) | 0.07 ± 0.04 (67%) | 0.02 ± 0.01 (49%) |
| m/z 43[c,e] | 0.4 ± 0.2 (56%) | 0.15 ± 0.06 (37%) | 0.12 ± 0.08 (64%) | 0.04 ± 0.02 (57%) |
| acetaldehyde[c] | 0.2 ± 0.1 (38%) | 0.11 ± 0.03 (30%) | 0.08 ± 0.04 (48%) | 0.02 ± 0.01 (51%) |
| m/z 57[c,f] | 0.6 ± 0.3 (47%) | 0.22 ± 0.08 (35%) | 0.2 ± 0.3 (120%) | 0.06 ± 0.03 (48%) |
| m/z 59[c,g] | 0.10 ± 0.05 (45%) | 0.04 ± 0.02 (43%) | 0.04 ± 0.03 (63%) | —— |
| higher alkenes[c,h] | 0.4 ± 0.2 (50%) | 0.15 ± 0.06 (41%) | 0.12 ± 0.07 (59%) | —— |
| m/z 73[c,i] | 0.07 ± 0.03 (39%) | 0.03 ± 0.01 (28%) | 0.03 ± 0.01 (55%) | 0.008 ± 0.004 (53%) |
| benzene[c] | 0.2 ± 0.1 (50%) | 0.08 ± 0.02 (29%) | 0.06 ± 0.03 (50%) | 0.015 ± 0.007 (46%) |
| m/z 83[c,j] | 0.13 ± 0.08 (63%) | 0.04 ± 0.01 (36%) | 0.03 ± 0.02 (66%) | 0.007 ± 0.004 (52%) |
| toluene[c] | 0.09 ± 0.05 (59%) | 0.02 ± 0.01 (51%) | 0.02 ± 0.02 (63%) | —— |
| phenol[c] | 0.09 ± 0.05 (59%) | 0.03 ± 0.01 (52%) | 0.02 ± 0.02 (76%) | —— |
| styrene[c] | 0.04 ± 0.02 (53%) | 0.015 ± 0.006 (41%) | 0.010 ± 0.005 (54%) | —— |
| m/z 107[c,k] | 0.12 ± 0.06 (51%) | 0.04 ± 0.02 (39%) | 0.03 ± 0.02 (67%) | 0.007 ± 0.005 (67%) |
| m/z 121[c,l] | 0.12 ± 0.07 (59%) | 0.04 ± 0.02 (46%) | 0.03 ± 0.02 (68%) | 0.008 ± 0.006 (73%) |
| m/z 135[c,l] | 0.08 ± 0.05 (65%) | 0.03 ± 0.01 (50%) | 0.02 ± 0.02 (74%) | 0.006 ± 0.005 (73%) |
| m/z 149[c,l] | 0.04 ± 0.03 (78%) | —— | 0.01 ± 0.01 (127%) | —— |
| naphthalene[c] | 0.03 ± 0.02 (51%) | 0.015 ± 0.007 (47%) | 0.01 ± 0.01 (80%) | 0.004 ± 0.003 (71%) |
| methyl naphthalene[c] | 0.02 ± 0.01 (61%) | 0.009 ± 0.004 (47%) | 0.007 ± 0.006 (81%) | 0.003 ± 0.002 (70%) |
| *Sum*[m] | 4.65 ± 0.73 (16%) | 1.76 ± 0.37 (21%) | 1.31 ± 0.49 (37%) | 0.28 ± 0.21 (75%) |

[a]measured by TDL-TILDAS; number of replicates: 53 (4%), 8 (5.5%), 72 (7%), 8 (15%)
[b]measured by QCL-TILDAS; number of replicates: 22 (4%), 4 (5.5%), 24 (7%), 4 (15%)
[c]measured by PTR-MS; number of replicates: 51 (4%), 8 (5.5%), 72 (7%), 8 (15%)
[d]fragment of propene
[e]propene and fragments of pentene isomers
[f]acrolein + butenes
[g]glyoxal + propanal + acetone
[h]sum of m/z 71, 85, 99, 113, and 127 representing pentene isomers through nonene isomers
[i]methyl glyoxal + butanal/crotonaldehyde
[j]possibly hexnal, cyclohexene, or hexadiene
[k]benzaldehyde + xylene
[l]variously substituted benzene isomers
[m]includes some high-uncertainty data indicated by a long dash in the table

idle, followed by formaldehyde (the most abundant on a simple molar basis), m/z 57 (acrolein + butenes), and m/z 43 (propene + fragments of petenes). These measurements show that the hydrocarbon emissions are dominated by carbonyls and olefins at idle power conditions where hydrocarbon emissions are most important.

The sum of the individual HC emissions measured by TILDAS and PTR-MS was compared with the total nonmethane hydrocarbons (NMHC) emissions data measured by NASA with a continuous flame-ionization detector (FID). Both techniques show that the hydrocarbon emissions decrease steeply with increasing engine power (see Fig. 6). The sum of the TILDAS/PTR-MS hydrocarbons agrees with the total NMHC measured by FID to within about 10%. The carbon emission ratio $ER_C$ is particularly useful for comparing speciated HC measurements to total HC measurements because the continuous FID is essentially a carbon-counting instrument. At higher engine powers ($\geq$ 30%), the signals are below the detection limit of the TILDAS and PTR-MS instruments, as operated at APEX.

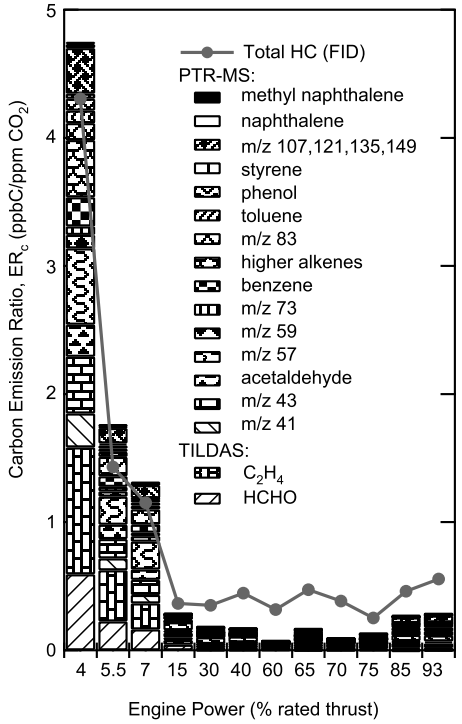


**Fig. 6 Comparison of sum of speciated hydrocarbons from TILDAS and PTR-MS with total hydrocarbon measurement from NASA continuous FID (all fuels; all downstream distances).**

### Engine-Related Hydrocarbon Emissions Variability

Because of the high time-resolution of the instruments, the 1 m probe measurements elucidated some interesting characteristics of the engine, which are discussed in the next two figures. Unlike the 10 and 30 m locations, wind has a negligible effect on the measurements at the 1 m probe, and so the variability at 1 m can be attributed to the engine itself.

Figure 7 shows a 3 min segment of 1 s HCHO and $CO_2$ data sampled from 1 m downstream of the engine while the engine was at the ICAO idle condition (7% engine power). The peaks in the $CO_2$ trace correspond quite well to the troughs in the HCHO trace, and it appears that the two signals are strongly anticorrelated. The HCHO concentration varies by approximately 10% during this interval, which results in a 10% or larger variability in the HCHO emission index. This high-frequency oscillation in $EI_{HCHO}$ was not obvious in

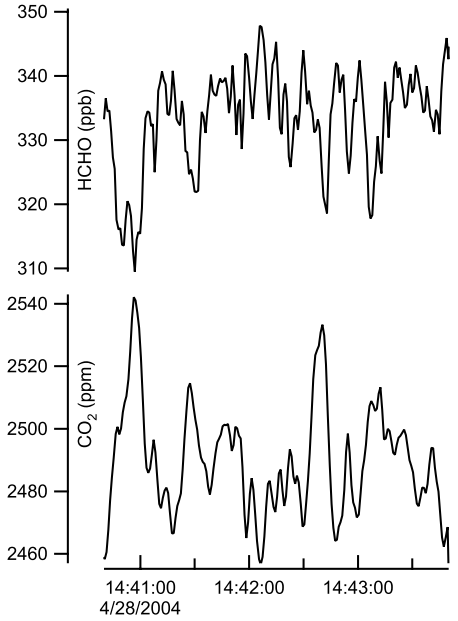


**Fig. 7 Variability in formaldehyde concentration sampled for a fixed engine condition.**

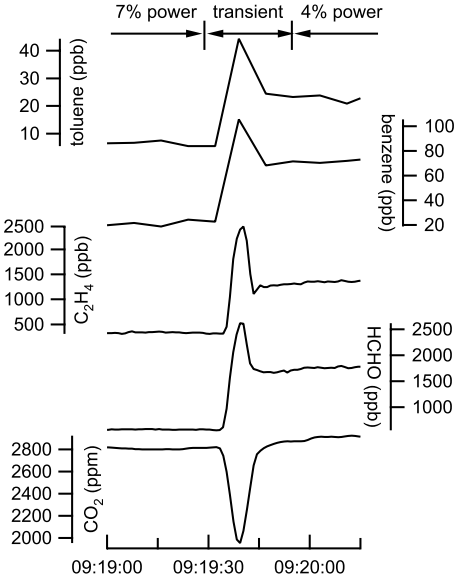


**Fig. 8 Hydrocarbon emissions during an engine power transient between ICAO idle and ground idle.**

all the 1 m probe data, and it is unclear what causes this variability. However, we believe the variability is engine-related rather than instrument/sampling-related because $CO_2$ and HCHO are measured on separate instruments and follow opposite trends. To our knowledge, this is the first time that this several-second variability in hydrocarbon emissions has been reported in the literature. Also, assuming HCHO emissions are indicative of total hydrocarbon emissions, the periods of low-HCHO and high-$CO_2$ emissions (e.g., 14:41:00) correspond to periods of relatively high combustion efficiency, and so there could be noticeable variability in the combustion efficiency of the engine on this several-second timescale.

The high time-response of the instruments (1 s for TILDAS, ~7 s for PTR-MS) also allowed the hydrocarbon emissions to be analyzed for transient engine powers between stable measurement points. Figure 8 shows the emissions of benzene, toluene, formaldehyde, ethylene, and $CO_2$ during a transition from 7% engine power (ICAO idle) to 4% engine power (ground idle), measured at 1 m downstream. During this 15 s transient period, the emission ratios for the four hydrocarbon species peak at a value that is approximately twice as high as the steady-state value for 4% engine power. Peaks for hydrocarbon emission indices were not observed for all changes in power conditions, and the degree of the excursion during the transient varied. Further measurements are needed to determine whether emissions during transient power conditions are consistently different from the emissions at steady-state power conditions bounding the transient powers levels.

## Conclusions

Emissions of formaldehyde, ethylene, acetaldehyde, benzene, toluene, and other hydrocarbons from a commercial high-bypass-ratio turbofan engine (CFM56-2C1) have been measured for various fuel formulations, plume ages (distances downstream), and engine powers using sensitive, fast time-response, trace gas analyzers. These speciated measurements provide information about the individual air toxics and greenhouse gases emitted by aircraft, and the sum of these speciated measurements agrees favorably with separate measurements of the total hydrocarbon emissions.

Fuel sulfur and aromatic content did not have a quantifiable effect on hydrocarbon emissions in the range studied (400–1600 ppmm sulfur, 18–22 vol % aromatics). Similarly, plume age (or distance downstream) did not have a quantifiable effect on hydrocarbon emissions in the range studied (1–30 m downstream of the engine-exit plane). Ambient temperature was shown to have a significant effect on hydrocarbon emissions, which obscured any lesser effects of fuel composition or plume age.

Hydrocarbon emission indices are highest at idle and decrease rapidly at higher engine powers. Variability in the measured emission index at a given nominal engine power was mostly due to variability in the ambient temperature, most likely through its impact on combustor-inlet temperature.

Fast time-response measurements of the individual hydrocarbon species emitted by the engine led to some interesting observations about the transient behavior of the engine. Variations in formaldehyde emissions ($\pm 10\%$) at 1 m downstream of the engine-exit plane were strongly anticorrelated with $CO_2$ emissions on a several-second timescale. Also, hydrocarbon emissions during transients in engine power were occasionally observed to be higher than the emissions in both the stable beginning and ending states.

## Acknowledgments

The authors would like to thank Chowen Wey (NASA John H. Glenn Research Center) and Phil Whitefield (University of Missouri–Rolla) for the opportunity to participate in the APEX measurement campaign. We are also grateful to Bruce Anderson (NASA Langley Research Center) for the high-range $CO_2$ data, and William Dodds (General Electric) for information about the combustor-inlet conditions. Finally, we are thankful to NASA Dryden Flight Research Center for providing the facilities for this experiment and to the whole APEX team for making this mission a success.

## References

[1] Anon., "ICAO Aircraft Engine Emissions Databank," International Civil Aviation Organization, http://www.caa.co.uk [retrieved Aug. 2005].

[2] Pison, I., and L. Menut, "Quantification of the Impact of Aircraft Traffic Emissions on Tropospheric Ozone over Paris Area," *Atmospheric Environment*, Vol. 38, No. 7, 2004, pp. 971–983.

[3] Yu, F. Q., Turco, R. P., and Karcher, B., "Possible Role of Organics in the Formation and Evolution of Ultrafine Aircraft Particles," *Journal of Geophysical Research [Atmospheres]*, Vol. 104, No. D4, 1999, pp. 4079–4087.

[4] Yu, K. N., Cheung, Y. P., Cheung, T., and Henry, R. C., "Identifying the Impact of Large Urban Airports on Local Air Quality by Nonparametric Regression," *Atmospheric Environment*, Vol. 38, No. 27, 2004, pp. 4501–4507.

[5] Spicer, C. W., Holdren, M. W., Smith, D. L., Hughes, D. P., and Smith,

M. D., "Chemical Composition of Exhaust from Aircraft Turbine Engines," *Journal of Engineering for Gas Turbines and Power*, Vol. 114, No. 1, 1992, pp. 111–17.

[6] Spicer, C. W., Holdren, M. W., Riggin, R. M., and Lyon, T. F., "Chemical Composition and Photochemical Reactivity of Exhaust from Aircraft Turbine Engines," *Annales Geophysicae*, Vol. 12, Nos. 10–11, 1994, pp. 944–55.

[7] Slemr, F., Giehl, H., Habram, M., Slemr, J., Schlager, H., Schulte, P., Haschberger, P., Lindermeir, E., Dopelheuer, A., and Plohr, M., "In-Flight Measurement of Aircraft CO and Nonmethane Hydrocarbon Emission Indices," *Journal of Geophysical Research [Atmospheres]*, Vol. 106, No. D7, 2001, pp. 7485–7494.

[8] Vay, S. A., Anderson, B. E., Sachse, G. W., Collins, J. E., Podolske, J. R., Twohy, C. H., Gandrud, B., Chan, K. R., Baughcum, S. L., and Wallio, H. A., "DC-8-Based Observations of Aircraft CO, $CH_4$, $N_2O$, and $H_2O$(g) Emission Indices During SUCCESS," *Geophysical Research Letters*, Vol. 25, No. 10, 1998, pp. 1717–1720.

[9] Anderson, B. E., Chen, G., and Blake, D. R., "Hydrocarbon Emissions from a Modern Commercial Airliner," *Atmospheric Environment*, Vol. 40, No. 19, 2006, pp. 3601–3612.

[10] Herndon, S. C., Rogers, T., Dunlea, E., Jayne, J., Miake-Lye, R., and Knighton, B., "Hydrocarbon Emissions from In-Use Commercial Aircraft During Airport Operations," *Environmental Science and Technology*, Vol. 40, No. 14, 2006, pp. 4406–4413.

[11] Wey, C. C., Anderson, B. E., Wey, C., Li-Jones, X., Winstead, E., Thornhill, L. K., Lobo, P., Hagen, D., Whitefield, P. D., Yelvington, P. E., Herndon, S. C., Onasch, T. B., Miake-Lye, R. C., and Wormhoudt, J., "Overview on the Aircraft Particle Emissions eXperiment (APEX)," *Journal of Propulsion and Power* (in this issue).

[12] Knighton, W. B., Rogers, T. M., Anderson, B. E., Herndon, S. C., Yelvington, P. E., and Miake-Lye, R. C., "Application of Proton Transfer Reaction Mass Spectrometry (PTR-MS) to Measurement of Volatile Organic Trace Gas Emissions from Aircraft," *Journal of Propulsion and Power* (in this issue).

[13] Wormhoudt, J., Herndon, S. C., Yelvington, P. E., Miake-Lye, R. C., and Wey, C., "Nitrogen Oxide ($NO/NO_2/HONO$) Emissions Measurements in Aircraft Exhausts," *Journal of Propulsion and Power* (in this issue).

[14] Onasch, T. B., Jayne, J., Herndon, S., Mortimer, P., Worsnop, D., and Miake-Lye, R. C., "Aircraft Particle Emissions eXperiment (APEX): Chemical Properties of Aircraft Engine Exhaust Aerosols Sampled During APEX (Appendix J)," NASA TM 2006-214382, Sept. 2006.

[15] Wey, C. C., Anderson, B. E., Hudgins, C., Wey, C., Li-Jones, X., Winstead, E., Thornhill, L. K., Lobo, P., Hagen, D., Whitefield, P., Yelvington, P. E., Herndon, S. C., Onasch, T. B., Miake-Lye, R. C., Wormhoudt, J., Knighton, W. B., Howard, R., Bryant, D., Corporan, E., Moses, C., Holve, D., and Dodds, W., "Aircraft Particle Emissions eXperiment (APEX)," NASA TM 2006-214382, Sept. 2006.

[16] Jimenez, R., Herndon, S. C., Shorter, J. H., Nelson, D. D., Jr., McManus, J. B., and Zahniser, M., "Atmospheric Trace Gas Measurements Using a Dual Quantum-Cascade Laser Mid-Infrared Absorption Spectrometer," *SPIE Proceedings*, Vol. 5738, Society of Photo-Optical Instrumentation, 2005, p. 318.

[17] Nelson, D. D., McManus, J. B., Urbanski, S., Herndon, S., and, Zahniser, M. S., "High Precision Measurements of Atmospheric Nitrous Oxide and Methane Using Thermoelectrically Cooled Mid-Infrared Quantum Cascade Lasers and Detectors," *Spectrochimica Acta, Part A (Molecular Spectroscopy)*, Vol. 60, No. 14, 2004, pp. 3325–3335.

[18] Herndon, S. C., Nelson, D. D., Li, Y., and Zahniser, M. S., "Determination of Line Strengths for Selected Transitions in the $\nu_2$ Band Relative to the $\nu_1$ and $\nu_5$ Bands of $H_2CO$," *Journal of Quantitative Spectroscopy and Radiative Transfer*, Vol. 90, No. 2, 2005, pp. 207–216.

[19] Rothman, L. S., Jacquemart, D., Barbe, A., Benner, C. D., Birk, M., Brown, L. R., Carleer, M. R., Chackerian, J. C., Chance, K., Coudert, L. H., Dana, V., Devi, V. M., Flaud, J.-M., Gamache, R. R., Goldman, A., Hartmann, J.-M., Jucks, K. W., Maki, A. G., Mandin, J.-Y., Massie, S. T., Orphal, J., Perrin, A., Rinsland, C. P., Smith, M. A. H., Tennyson, J., Tolchenov, R. N., Toth, R. A., Vander Auwera, J., Varanasi, P., and Wagner, G., "HITRAN 2004 Molecular Spectroscopic Database," *Journal of Quantitative Spectroscopy and Radiative Transfer*, Vol. 96, No. 2, 2005, pp. 139–204.

[20] Smith, M. A. H., Rinsland, C. P., Fridovich, B., and Rao, K. N., "Intensites and Collision Broadening Parameters from Infrared Spectra," *Molecular Spectroscopy: Modern Research*, Academic Press, New York, 1985, Chap. 3.

[21] Anderson, B. E., Cofer, W. R., Bagwell, D. R., Barrick, J. D., Hudgins, C. H., and Brunke, K. E., "Airborne Observations of Aircraft Aerosol Emissions 1: Total Nonvolatile Particle Emission Indices," *Geophysical Research Letters*, Vol. 25, No. 10, 1998, pp. 1689–1692.

[22] Fahey, D. W., Keim, E. R., Boering, K. A., Brock, C. A., Wilson, J. C., Jonsson, H. H., Anthony, S., Hanisco, T. F., Wennberg, P. O., Miake-Lye, R. C., Salawitch, R. J., Louisnard, N., Woodbridge, E. L., Gao, R. S., Donnelly, S. G., Wamsley, R. C., Del Negro, L. A., Solomon, S., Daube, B. C., Wofsy, S. C., Webster, C. R., May, R. D., Kelly, K. K., Loewenstein, M., Podolske, J. R., and Chan, K. R., "Emission Measurements of the Concorde Supersonic Aircraft in the Lower Stratosphere," *Science*, Vol. 270, No. 5233, 1995, pp. 70–74.

[23] Schäfer, K., Jahn, C., Sturm, P., Lechner, B., and Bacher, M., "Aircraft Emission Measurements by Remote Sensing Methodologies at Airports," *Atmospheric Environment*, Vol. 37, No. 37, 2003, pp. 5261–5271.

[24] Herndon, S. C., Shorter, J. H., Zahniser, M. S., Nelson, D. D., Jayne, J., Brown, R. C., Miake-Lye, R. C., Waitz, I., Silva, P., Lanni, T., Demerjian, K., and Kolb, C. E., "NO and $NO_2$ Emission Ratios Measured from In-Use Commercial Aircraft During Taxi and Takeoff," *Environmental Science and Technology*, Vol. 38, No. 22, 2004, pp. 6078–6084.

L. Maurice
*Associate Editor*